Available online at www.sciencedirect.com
ScienceDirect
Carbohydrate Research 341 (2006) 2803–2815
Carbohydrate RESEARCH

Complete assignment of hyaluronan oligosaccharides up to hexasaccharides

Charles D. Blundell,[a] Michelle A. C. Reed[b] and Andrew Almond[a,*]

[a]*Faculty of Life Sciences, Manchester Interdisciplinary Biocentre, University of Manchester, Princess Street, Manchester M1 7DN, UK*
[b]*The Henry Wellcome Building for Biomolecular NMR Spectroscopy, CR-UK Institute for Cancer Studies, University of Birmingham, Vincent Drive, Edgbaston, Birmingham B15 2TT, UK*

Received 31 July 2006; received in revised form 18 September 2006; accepted 27 September 2006
Available online 4 October 2006

Abstract—The glycosaminoglycan hyaluronan is involved in a diverse range of physiological and diseases processes and comprises repeated disaccharide units of *N*-acetyl-D-glucosamine (GlcNAc) and D-glucuronic acid (GlcA). A molecular description of the solution conformation of HA is required to account for this biology, which is best attained using nuclear magnetic resonance (NMR). NMR studies of the polymer, however, are frustrated by resonance overlap arising from the highly degenerate structure. In contrast, end-effects in oligosaccharides can produce some chemical shift dispersion, giving the possibility that their conformational properties can be measured and extrapolated to models of the polymer. We report the complete resolution and assignment of ^{1}H, ^{13}C and ^{15}N nuclei in hyaluronan oligosaccharides with seven different naturally occurring terminal rings. At 900 MHz, all ^{1}H nuclei in the hexasaccharide GlcA-β-(1→3)-GlcNAc-β-(1→4)-GlcA-β-(1→3)-GlcNAc-β-(1→4)-GlcA-β-(1→3)-GlcNAc-OH were uniquely resolved and the two central rings were found to be a good model for the polymer environment. These assignments now allow resolved, unambiguous structural restraints to be acquired on this oligosaccharide and extrapolated to models for the solution conformation of the polymer.

Keywords: Hyaluronan; Strong coupling; Coupling constant; End-effect; Resolution

1. Introduction

Hyaluronan (HA) is a glycosaminoglycan composed of a repeated disaccharide of *N*-acetyl-D-glucosamine (GlcNAc) and D-glucuronic acid (GlcA). Amidst many other functions, it provides structural integrity and organisation to vertebrate extracellular matrices.[1,2] The polymer is involved in both physiological (e.g., cervical ripening,[3] tooth development[4]) and disease processes (e.g., endometrial cancer,[5] atherosclerosis[6]), while HA oligosaccharides have distinct activities under some conditions (e.g., inducing dendritic cell maturation).[7] To understand the molecular basis of these processes, characterization of the physical properties and structures of the polymer and oligosaccharides is required. In this regard, hydrodynamic and nuclear magnetic resonance (NMR) data indicate that polymeric HA behaves as a stiffened, worm-like coil in solution, with significant dynamic motions at the glycosidic linkages.[8]

The degenerate chemical structure of HA results in poor NMR chemical-shift dispersion (particularly of the ^{1}H nuclei),[9,10] making the assignment and acquisition of structural data (which typically involves ^{1}H nuclei) difficult. The high viscosity of polymeric HA preparations broadens resonance linewidths and limits

Abbreviations: DQF-COSY, double quantum-filtered correlation spectroscopy; DSS, dimethyl-2-silapentane-5-sulfonate; GlcA, D-glucuronic acid; GlcNAc, *N*-acetyl-D-glucosamine; HA, hyaluronan; HSQC, heteronuclear single quantum correlation; NOE, nuclear Overhauser enhancement; NOESY, NOE spectroscopy; RDC, residual dipolar coupling; ROE, rotating frame NOE; TOCSY, total correlation spectroscopy.

* Corresponding author. Tel.: +44 161 30 64 199; fax: +44 161 306 8918; e-mail: andrew.almond@manchester.ac.uk

0008-6215/$ - see front matter © 2006 Elsevier Ltd. All rights reserved.
doi:10.1016/j.carres.2006.09.023

the concentration achievable, rendering many experiments unfeasible.[11] In contrast, oligosaccharide preparations can be made at high concentrations without problematic viscosity, and therefore provide a good model system for structural studies on the polymer. Moreover, different chemical structures and environments associated with terminal rings provide some chemical shift differences at the termini relative to interior rings, which are termed 'end-effects'. Chemically distinct structures in HA oligosaccharide terminal rings that can produce a variety of end-effects include the lack of one glycosidic linkage relative to interior rings, the presence of different terminal rings at each end (e.g., GlcA, GlcNAc) and mutarotation in reducing terminal rings generating α- and β-anomers. In addition to the different chemical shifts inherent to these different chemistries, these different structures also result in altered local environments (e.g., dynamic motions, water structuring) causing chemical shift perturbations in penultimate rings, even though they are in an identical chemical structure to more interior ones.[9,10,12,13] Crucially, the chemical shift dispersion generated by these end-effects facilitates the measurement of structural restraints at sequence-specific positions.[14] Because the central residues in oligosaccharides are less subject to these end-effects, they progressively approach the environment of the polymer as the chain is lengthened.[10,15] Consequently, it is desirable to achieve resolved, sequence-specific ^{1}H assignments in the centre of as long a length of HA oligosaccharide as possible so that the average conformation and spread of the glycosidic linkages can be measured precisely. Such measurements can then be extrapolated to models of the polymer.[16]

End-effects in tetrasaccharides (HA_4^{AN}, molecule **5** in Fig. 1) have allowed complete sequence-specific ^{1}H assignment at 600 MHz,[9,12] although some assignments are still in dispute due to the lack of resolution at this field.[9] However, end-effects are significant at the central residues in this oligosaccharide,[10,15] meaning that it is a poor approximation to the polymer. Sequence-specific ^{1}H assignment and resolution in longer oligosaccharides is therefore crucial if structural data measured on oligosaccharides are to be usefully extrapolated to models of the polymer. In this regard, the sensitivity of ^{15}N nuclei to end-effects in ^{15}N-labelled HA oligosaccharides has been shown to allow resolution and assignment of the central amide H^N groups in oligosaccharides as long as the decasaccharides (HA_{10}^{AN}).[15] In further studies with ^{15}N-labelling, sequence-specific structural data have been acquired for the central residues in octasaccharides (HA_8^{AN}) and have been used to generate models for the polymer.[16,17]

To exploit the resolution of chemical shifts arising from end-effects further, we have recently developed protocols for the generation of all odd- and even-numbered HA oligosaccharides.[18] Consequently, the resolution attainable by end-effects from three different non-reducing terminal residues (GlcA, GlcNAc, Δ-4,5-GlcA)

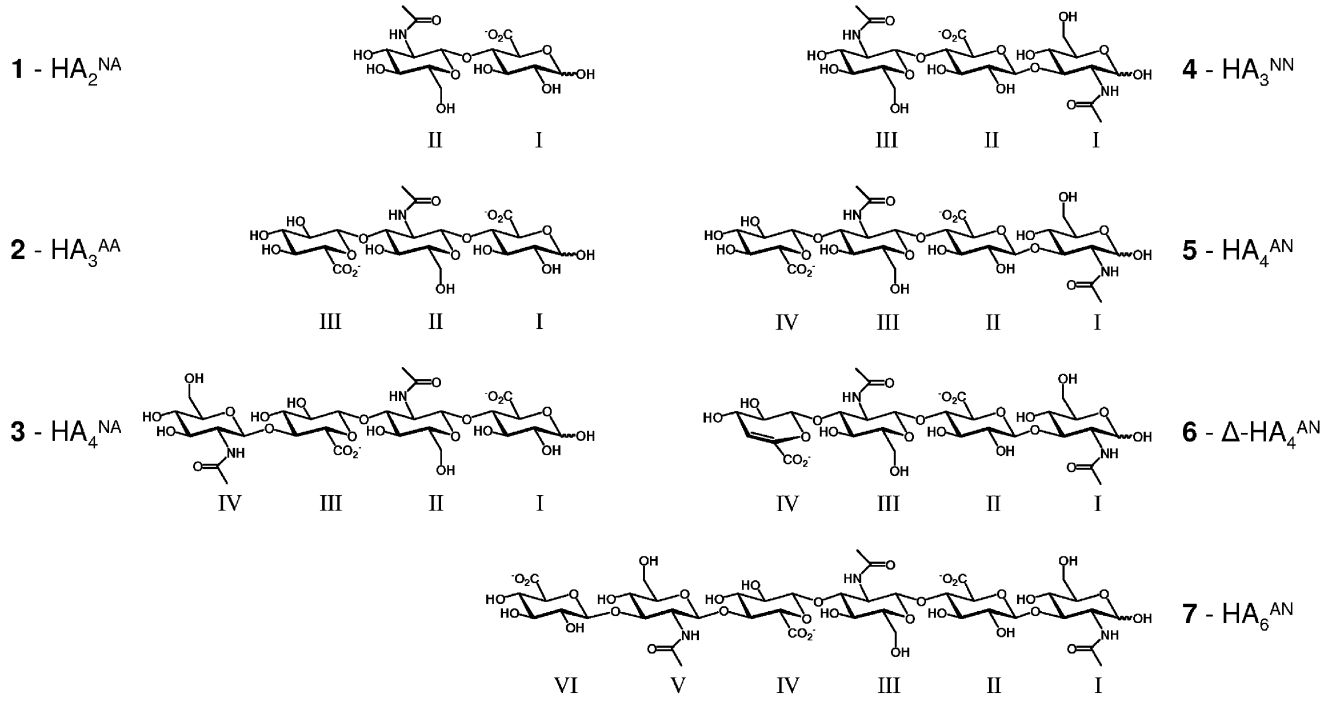

Figure 1. HA oligosaccharides for which ring ^{1}H and ^{13}C nuclei were assigned in this work. The oligosaccharide designation HA_X^{YZ} details each structure, where X refers to the number of saccharide residues, Y the residue at the non-reducing terminus (A for GlcA, N for GlcNAc) and Z the residue at the reducing terminus.[18] Ring numbers in roman numerals are given from the reducing terminus.

and four different reducing terminal residues (α- and β-anomers of both GlcA and GlcNAc) can now be examined. In addition, we have shown that the spectra recorded on oligosaccharides at 900 MHz have an extra resolution enhancement due to their fortuitous molecular tumbling rate.[19]

In this work we report the assignments of all ^{1}H, ^{13}C and ^{15}N nuclei within a range of HA oligosaccharides (**1**–**7**, Fig. 1), determined at 900 MHz using standard natural-abundance experiments. The end-effects from seven types of terminal ring are represented within this set and their potential use in achieving resolution in as long a length of HA oligosaccharide as possible is discussed. Ring ^{1}H and ^{13}C chemical shifts at the centre of the hexasaccharide **7** (HA_6^{AN}) are a good representation of those in the polymer, while the doicosasaccharide (HA_{22}^{AN}) is used to confirm previous work[15] that proposed acetamido groups at the center of an octasaccharide (HA_8^{AN}) represent the polymer well. Sequence-specific one-bond $^{1}J_{C,H}$ and vicinal coupling constants ($^{3}J_{H,H}$) are accurately measured within a range of oligosaccharides. This work provides a foundation set of experiments and data that will allow many sequence-specific structural restraints to be resolved unambiguously within the centre of the hexasaccharide **7** (HA_6^{AN}). These advances pave the way to successful characterization of the solution conformation of the polymer and hence a molecular understanding of its roles in both physiological and disease processes.

2. Results

2.1. Assignment of HA oligosaccharides 1–7

Complete assignment of all ^{1}H and ^{13}C chemical shifts (except carbonyl and carboxyl ^{13}C) within HA oligosaccharides **1**–**7** was achieved at 900 MHz, pH 6.0 and 24.4 °C using [^{1}H–^{1}H]-DQF-COSY, [^{1}H–^{1}H]-Z-filtered-TOCSY, [^{1}H–^{1}H]-NOESY and [^{1}H–^{13}C]-HSQC spectra (Tables 1–3). The resolution obtained at this field-strength was sufficient to clearly resolve every ^{1}H and ^{13}C nucleus in at least one spectrum, even in the case of the hexasaccharide **7** (HA_6^{AN}); resonance assignments for the most overlapped portion of the [^{1}H–^{1}H]-DQF-COSY and [^{1}H–^{1}H]-Z-filtered-TOCSY spectra of **6** (Δ-HA_4^{AN}) are shown in Supplementary data (Supplementary Fig. 1). Amide ^{1}H (i.e., H^{N}) and ^{15}N chemical shifts for **1**–**7** and longer oligosaccharides (Table 4) were assigned by comparison of resonances in [^{1}H–^{15}N]-HSQC spectra (recorded at 750 MHz) for oligosaccharides with different residue compositions.[15,18]

While much of the assignment of GlcA and GlcNAc rings became routine at such high fields, a few points of interest are noted here. Low intensity resonances arising from partial evolution of $^{2}J_{CH}$ couplings (≈5 Hz) were frequently observed in [^{1}H–^{13}C]-HSQC spectra and considerably aided the interpretation of [^{1}H–^{1}H]-DQF-COSY spectra (i.e., [^{1}H–^{13}C]-HMBC spectra were not needed). These peaks were also useful in allowing the accurate measurement of ^{13}C chemical shifts where the $^{1}J_{CH}$ peak was occluded by spectral overlap; for example, the C-5 chemical shifts of rings Iβ, III and V in the hexasaccharide **7** (HA_6^{AN}) were discriminated in this way. In a few cases where the $^{1}J_{CH}$ and $^{2}J_{CH}$ resonances overlapped (e.g., at H-3, C-3^{VI} and H-4, C-3^{VI} in **7**), the [^{1}H–^{13}C]-HSQC spectrum recorded without broadband ^{13}C-decoupling during acquisition allowed the two resonances to be separated, because the difference between the two couplings is quite different ($^{1}J_{CH} \approx 150$ Hz, $^{2}J_{CH} \approx 5$ Hz). H6*proR* and H6*proS* were assigned by their 3-bond coupling constants to H-5 (Table 5, Fig. 2). As in D-GlcNAc, H6*proS* always has the higher chemical shift in HA oligosaccharides.[20]

Determination of the location of each GlcA and GlcNAc spin system within each oligosaccharide was initially achieved by comparison of the assignments made for the di- and trisaccharides (**1**, **2**, **4**) with progressively longer chains until the hexasaccharide **7** was reached. These sequential assignments were confirmed using sequence-specific NOEs to each GlcNAc N–H proton from the H-1 proton of the adjacent β-(1→3)-linked GlcA (all N–H and H-1 protons have distinctive chemical shifts in oligosaccharides **1**–**7**).[11,16,17] Assignment of the H–Me chemical shift of each acetamido sidechain was initially achieved by observation of NOEs to GlcNAc N–H protons. Because the ^{15}N-chemical shifts are distinctive for short HA oligosaccharides (see Table 4), a modified [^{1}H–^{15}N]-HSQC spectrum exploiting the very small $^{3}J_{H-Me,N}$ coupling (value not determined) was also used to correlate each H–Me group to its corresponding acetamido ^{15}N nucleus (see Supplementary Fig. 2).

The α:β anomer ratio for oligosaccharides with reducing terminal GlcNAc and GlcA residues was measured by comparison of peak volumes of resonances distinctive for α and β forms. As determined from the Iα and Iβ [H–Me^{I},C–Me^{I}] resonances in the [^{1}H–^{13}C]-HSQC spectrum, the reducing terminal GlcNAc ring in HA oligosaccharides comprises 60.4 ± 0.7% α-anomer at pH 6.0 and 24.4 °C (irrespective of oligosaccharide length); this value is not discernibly different from GlcNAc monosaccharide. A reducing terminal GlcA ring, as assessed by the ratio of volumes of the IIα and IIβ [H–N^{II},N^{II}] resonances in the [^{1}H–^{15}N]-HSQC, comprises 42.7 ± 0.7% α-anomer at pH 6.0 and 24.4 °C; this value is also not discernibly different from GlcA monosaccharide.[13]

The chemical shifts of resonances relative to internal DSS (δ_{DSS}) were found to be very consistent between different samples of the same oligosaccharide (at the same temperature, D_2O concentration and pH),

Table 1. ^{1}H and ^{13}C chemical shifts for HA oligosaccharides with GlcA at the reducing terminus

		1–HA_2^{NA}		**2**–HA_3^{AA}		**3**–HA_4^{NA}	
		α	β	α	β	α	β
I—GlcA 1	H-1	5.203[a]	4.626	5.196	4.620	5.200	4.622
	H-2	3.599	3.300	3.596	3.299	3.597	3.298
	H-3	3.761	3.574	3.760	3.573	3.759	3.573
	H-4	3.710	3.735	3.717	3.742	3.710	3.735
	H-5	4.069	3.710	4.065	3.707	4.060	3.701
II—GlcNAc	H-1	4.527	4.522	4.565	4.560	4.546	4.544
	H-2	3.694	3.699	3.843		3.838	
	H-3	3.520		3.710		3.708	
	H-4	3.459		3.539		3.520	
	H-5	3.460		3.482		3.478	
	H-6*proR*	3.763		3.775		3.767	
	H-6*proS*	3.926		3.920		3.916	
	H–Me	2.043		2.025		2.017	
III—GlcA	H-1			4.458		4.456	
	H-2			3.317		3.344	
	H-3			3.492		3.575	
	H-4			3.494		3.732	
	H-5			3.720		3.706	
IV—GlcNAc	H-1					4.521	
	H-2					3.692	
	H-3					3.515	
	H-4					3.454	
	H-5					3.455	
	H-6*proR*					3.756	
	H-6*proS*					3.917	
	H–Me					2.043	
I—GlcA I	C-1	94.886	98.939	94.773	98.842	94.893	98.959
	C-2	74.035	76.681	73.843	76.482	74.023	76.671
	C-3	73.795	76.675	73.670	76.552	73.796	76.674
	C-4	83.019	82.756	83.145	82.878	83.172	82.896
	C-5	74.766	79.490	74.780	79.513	74.788	79.507
II—GlcNAc	C-1	103.479	103.380	103.311	103.209	103.316	103.224
	C-2	58.212		56.950		57.110	
	C-3	76.725	76.811	85.791		85.304	
	C-4	72.582		71.275		71.266	
	C-5	78.662		78.160		78.143	
	C-6	63.410		63.285		63.395	
	C–Me	25.232		25.212		25.318	
III—GlcA	C-1			105.714		105.877	
	C-2			75.440		75.360	
	C-3			78.049		76.431	
	C-4			74.432		82.552	
	C-5			78.457		79.013	
IV—GlcNAc	C-1					103.428	
	C-2					58.230	
	C-3					76.775	
	C-4					72.562	
	C-5					78.660	
	C-6					63.388	
	C–Me					25.242	

[a] All chemical shifts were measured at pH 6.0, 24.4 °C for oligosaccharides in 5–10% (v/v) D_2O (except for **2** which was in 100% D_2O) and referenced relative to $\delta_{DSS}(^{1}H)$. Standard errors: ^{1}H ±0.001 ppm, ^{13}C ±0.004 ppm.

giving very low standard errors ($\delta_{DSS}(^{1}H)$ ±1 ppb; $\delta_{DSS}(^{13}C)$ ±4 ppb; $\delta_{DSS}(^{15}N)$ ±3 ppb). Perturbations to ^{1}H chemical shifts by one-bond ^{15}N or ^{13}C isotope-effects were approximately −2 to −3 ppb from those reported in the tables (i.e., those for ^{14}N and ^{13}C-bonded hydrogen atoms). The differences in chemical shifts for **2** (HA_3^{AA}) relative to similar residues in other oligosaccharides (e.g., comparing ring I in **1**, **2** and **3**; Table 1),

Table 2. ^{1}H and ^{13}C chemical shifts for HA oligosaccharides with GlcNAc at the reducing terminus

		4–HA_3^{NN}		**5**–HA_4^{AN}		**6**–Δ-HA_4^{AN}	
		α	β	α	β	α	β
I—GlcNAc	H-1	5.154[a]	4.715	5.155	4.713	5.154	4.713
	H-2	4.035	3.804	4.034	3.806	4.035	3.805
	H-3	3.887	3.714	3.890	3.716	3.889	3.715
	H-4	3.549	3.516	3.552	3.514	3.550	3.518
	H-5	3.866	3.472	3.869	3.472	3.867	3.468
	H-6*proR*	3.793	3.748	3.792	3.750	3.794	3.751
	H-6*proS*	3.826	3.890	3.827	3.890	3.828	3.891
	H–Me	2.013	2.015	2.014	2.015	2.012	2.014
II—GlcA	H-1	4.505	4.464	4.507	4.467	4.507	4.466
	H-2	3.363	3.363	3.366	3.363	3.365	3.365
	H-3	3.582	3.577	3.585	3.580	3.582	3.577
	H-4	3.740	3.738	3.748	3.744	3.745	3.743
	H-5	3.714	3.704	3.712	3.703	3.717	3.707
III—GlcNAc	H-1	4.524		4.560		4.579	
	H-2	3.695		3.851		3.846	
	H-3	3.518		3.707		3.805	
	H-4	3.458		3.542		3.506	
	H-5	3.458		3.484		3.504	
	H-6*proR*	3.757		3.780		3.774	
	H-6*proS*	3.919		3.921		3.921	
	H–Me	2.044		2.028		2.058	
IV—GlcA	H-1			4.458		5.147	
	H-2			3.321		3.744	
	H-3			3.496		4.135	
	H-4			3.497		5.849	
	H-5			3.723			
I—GlcNAc	C-1	93.877	97.582	93.879	97.589	93.878	97.587
	C-2	55.806	58.452	55.817	58.454	55.813	58.453
	C-3	82.800	85.206	82.758	85.151	82.774	85.170
	C-4	71.394	71.356	71.390	71.351	71.395	71.357
	C-5	74.073	78.261	74.080	78.264	74.078	78.264
	C-6	63.394	63.562	63.398	63.567	63.397	63.565
	C–Me	24.817	25.067	24.814	25.065	24.815	25.065
II—GlcA	C-1	105.658	105.810	105.675	105.818	105.659	105.805
	C-2	75.339	75.308	75.324	75.294	75.328	75.291
	C-3	76.491		76.506		76.522	
	C-4	82.628		82.781		82.820	
	C-5	79.070		79.098		79.057	
III—GlcNAc	C-1	103.489		103.325		103.160	
	C-2	58.218		57.049		57.474	
	C-3	76.738		85.839		85.044	
	C-4	72.552		71.357		71.197	
	C-5	78.650		78.183		78.350	
	C-6	63.374		63.390		63.418	
	C–Me	25.239		25.326		25.277	
IV—GlcA	C-1			105.715		103.496	
	C-2			75.578		72.681	
	C-3			78.213		68.953	
	C-4			74.560		110.070	
	C-5			78.477			

[a] All chemical shifts were measured at pH 6.0, 24.4 °C for oligosaccharides in 5–10% (v/v) D_2O and referenced relative to $\delta_{DSS}(^{1}H)$. Standard errors: ^{1}H ±0.001 ppm, ^{13}C ±0.004 ppm.

are principally due to deuterium isotope-effects arising from exchange of hydroxyl hydrogens for deuterons (this sample contained 100% D_2O whereas the others comprised 5–10% D_2O). Although a range of sample concentrations was used for oligosaccharides **1**–**7**, no chemical shift differences were seen for any oligosaccharide as its concentration varied over the range 0.1–35 mM, indicating that they do not significantly

Table 3. ^{1}H, ^{13}C chemical shifts and $^{1}J_{C,H}$ couplings constants for **7** (HA_6^{AN})

	Nucleus	α	β	Nucleus	α	β	$^{1}J_{CH}$	
I—GlcNAc	H-1	5.155[a]	4.711	C-1	93.880	97.593	172.0	162.7
	H-2	4.032	3.805	C-2	55.824	58.452	141.1	140.6
	H-3	3.889	3.714	C-3	82.735	85.126	—[b]	—
	H-4	3.546	3.513	C-4	71.395	71.348	—	148.4
	H-5	3.867	3.468	C-5	74.083	78.264	146.7	—
	H-6*proR*	3.792	3.749	C-6	63.398	63.566	—	—
	H-6*proS*	3.827	3.891				144.6	145.2
	H–Me	2.012	2.014	C–Me	24.818	25.068	129.2	129.2
II—GlcA	H-1	4.506	4.463	C-1	105.675	105.817	163.8	163.7
	H-2	3.363	3.363	C-2	75.321	75.282	146.0	146.0
	H-3	3.582	3.578	C-3	76.500	76.500	144.7	144.7
	H-4	3.745	3.741	C-4	82.777	82.777	148.6	148.6
	H-5	3.708	3.699	C-5	79.114	79.114	148.5	148.2
III—GlcNAc	H-1	4.548		C-1	103.323		163.9	
	H-2	3.839		C-2	57.120		142.3	
	H-3	3.707		C-3	85.323		144.2	
	H-4	3.519		C-4	71.244		148.7	
	H-5	3.476		C-5	78.126		—	
	H-6*proR*	3.764		C-6	63.367		—	
	H-6*proS*	3.910					145.9	
	H–Me	2.021		C–Me	25.327		129.2	
IV—GlcA	H-1	4.457		C-1	105.899		163.9	
	H-2	3.344		C-2	75.349		145.8	
	H-3	3.577		C-3	76.435		144.8	
	H-4	3.736		C-4	82.688		148.5	
	H-5	3.704		C-5	79.023		148.3	
V—GlcNAc	H-1	4.554		C-1	103.268		163.8	
	H-2	3.843		C-2	57.050		142.3	
	H-3	3.705		C-3	85.886		144.1	
	H-4	3.539		C-4	71.351		—	
	H-5	3.477		C-5	78.187		—	
	H-6*proR*	3.776		C6	63.391		—	
	H-6*proS*	3.918					—	
	H–Me	2.027		C–Me	25.327		129.2	
VI—GlcA	H-1	4.455		C-1	105.730		163.4	
	H-2	3.319		C-2	75.581		145.9	
	H-3	3.495		C-3	78.210		143.7	
	H-4	3.496		C-4	74.560		147.3	
	H-5	3.722		C-5	78.459		145.4	

[a] All chemical shifts for **7** were measured at pH 6.0, 24.4 °C in 5–10% (v/v) D_2O and referenced relative to $\delta_{DSS}(^{1}H)$. Standard errors: ^{1}H ±0.001 ppm, ^{13}C ±0.003 ppm, $^{1}J_{CH}$ ±0.2 − 0.5 Hz.
[b] Value not determined.

self-associate under these conditions (the presence of other species at <1% can be easily detected at the signal-to-noise ratios routinely used).[18]

2.2. Coupling constants and strong-coupling within HA oligosaccharides

Having completed the assignment of ^{1}H and ^{13}C nuclei within **7** (HA_6^{AN}), one-bond $^{1}J_{C,H}$ coupling constants were directly measured for the C–H groups from a [^{1}H–^{13}C]-HSQC spectrum recorded with ^{13}C-broadband decoupling disabled during acquisition (see Table 4 and Supplementary Fig. 3). All $^{1}J_{C,H}$ values are typical of saccharide rings.[21] The $^{1}J_{C1,H1}$ values, which are characteristic for α- and β-arrangements, are very similar to those found in GlcNAc monosaccharide[22] and heparin oligosaccharides.[21,23]

Vicinal $^{3}J_{H,H}$ coupling constants were directly measured from very high-resolution 1D spectra of the monosaccharide GlcNAc and oligosaccharides **1**, **2**, **3** and **5** (see Table 5). In spite of the narrow spectral range over which most resonances occur (i.e., 3.3–3.9 ppm), it was possible to measure almost all the $^{3}J_{H,H}$ couplings directly from the 1D spectra (even within the tetrasaccharide **5**). The ring $^{3}J_{H,H}$ couplings in HA oligosaccharides are very similar to those found in monosaccharide GlcA and GlcNAc, indicating that the residues adopt the same conformation (i.e., $^{4}C_1$ chairs).[13,22] The

Table 4. ^{1}H and ^{15}N chemical shifts for oligosaccharides **1**–**7** and longer lengths

Ring	Iα	Iβ	III	V	VII	Iα	Iβ	III	V	VII
GlcNAc at reducing terminus										
GlcNAc[a]	8.071[b]	8.172				123.706	122.947			
5, HA_4^{AN}	8.188	8.271	8.055			122.943	122.089	122.134		
7, HA_6^{AN}	8.189	8.271	8.052	8.042		122.947	122.098	121.996	122.097	
HA_8^{AN}	8.191	8.271	8.052	8.042	8.042	122.953	122.101	121.996	121.954	122.097
6, $\Delta\text{-}HA_4^{AN}$	8.192	8.272	8.141			122.946	122.083	122.218		
$\Delta\text{-}HA_6^{AN}$	8.192	8.273	8.054	8.129		122.949	122.094	121.994	122.175	
$\Delta\text{-}HA_8^{AN}$	8.192	8.274	8.053	8.043	8.130	122.950	122.098	121.993	121.955	122.166
4, HA_3^{NN}	8.188	8.272	7.949			122.941	122.084	122.867		
HA_5^{NN}	8.189	8.271	8.050	7.941		122.950	122.097	122.006	122.840	
HA_7^{NN}	8.191	8.271	8.053	8.040	7.938	122.956	122.099	122.002	121.972	122.834
GlcA at reducing terminus										
	IIα	IIβ	IV	VI		IIα	IIβ	IV	VI	
1, HA_2^{NA}	7.944	7.938				122.832	122.846			
3, HA_4^{NA}	8.044	8.043	7.943			121.959	121.981	122.842		
HA_6^{NA}	8.042	8.045	—[c]	7.938		121.980	121.990	—	122.838	
2, HA_3^{AA}	8.048	8.049				122.093	122.116			
HA_5^{AA}	8.045	8.045	8.045			121.949	121.973	122.105		

[a] Values for monosaccharide GlcNAc.
[b] All chemical shifts were measured at pH 6.0, 24.4 °C in 5–10% (v/v) D_2O and referenced relative to $\delta_{DSS}(^{1}H)$. Standard errors: ^{1}H ±0.001 ppm, ^{15}N ±0.003 ppm.
[c] Value not determined.

Table 5. $^{3}J_{H,H}$ coupling constants within selected HA oligosaccharides

		$^{3}J_{1,2}$	$^{3}J_{2,3}$	$^{3}J_{3,4}$	$^{3}J_{4,5}$	$^{3}J_{5,6proR}$	$^{3}J_{5,6proS}$	$^{3}J_{6proR,6proS}$	$^{3}J_{2,H-N}$
GlcNAc rings									
GlcNAc[a]	Iα	3.60[b]	10.74	9.03	10.25	5.21	2.31	−12.34	8.88
	Iβ	8.46	10.40	8.80	—[c]	5.57	1.85	−12.30	9.07
1, HA_2^{NA}	IIα	8.46	10.31	8.83	s/c[d]	—	—	—	9.45
	IIβ	8.46	10.34	8.83	s/c	5.21	2.41	−12.25	9.40
2, HA_3^{AA}	IIα	8.55	10.33	8.75	9.92	5.34	2.28	−12.50	9.76
	IIβ	8.56	10.33	8.75	9.92	5.43	2.23	−12.50	9.78
3, HA_4^{NA}	IIα	8.61	10.30	8.71	9.92	5.35	2.26	−12.38	9.73
	IIβ	8.61	10.30	8.71	9.92	5.35	2.26	−12.38	9.73
	IV	8.46	10.25	8.74	s/c	—	—	−12.46	9.47
5, HA_4^{AN}	Iα	3.52	10.56	8.79	10.06	4.86	2.29	−12.46	9.47
	Iβ	8.41	—	8.81	9.73	5.47	2.20	−12.37	9.70
	III	8.57	10.37	—	10.00	5.32	2.31	−12.43	9.68
GlcA rings									
1, HA_2^{NA}	Iα	3.78	9.70	8.95	9.74				
	Iβ	7.96	9.47	8.60	9.70				
2, HA_3^{AA}	Iα	3.80	9.65	8.88	9.64				
	Iβ	8.00	9.40	8.78	9.69				
	III	7.83	9.50	s/c	9.65				
3, HA_4^{NA}	Iα	3.77	9.67	—	9.71				
	Iβ	7.97	9.45	8.79	9.78				
	III	7.83	9.47	—	9.68				
5, HA_4^{AN}	IIα	7.91	9.46	8.76	9.67				
	IIβ	7.92	9.46	8.76	9.67				
	IV	7.80	9.29	s/c	9.78				

[a] Values for monosaccharide GlcNAc.
[b] Standard error on all couplings ±0.05 Hz.
[c] Value not determined.
[d] Nuclei are strongly coupled.

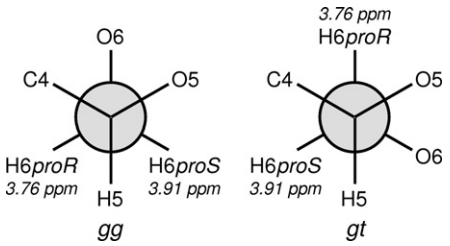

Figure 2. Newman projections for the *gg* and *gt* hydroxymethyl exocyclic conformations. The first letter describes the O-5–C-5–C-6–O-6 torsional angle, while the second the C-4–C-5–C-6–O-6 angle; *g* denotes *gauche* (60°) and *t trans* (180°). The observed $^{3}J_{H5,H6proS}$ (2.3 Hz) and $^{3}J_{H5,H6proR}$ (5.4 Hz) coupling constants reflect the relative proportions of *gg* and *gt* conformations present.[24]

$^{3}J_{H5,H6proR}$ and $^{3}J_{H5,H6proS}$ couplings in HA oligosaccharides (5.4 and 2.3 Hz, respectively) are, however, slightly different from β-GlcNAc (5.6 and 1.9 Hz). According to the relation of Hasnoot et al.,[24] these values correspond to hydroxymethyl fractional rotamer populations of 47% *gg* and 53% *gt* in HA oligosaccharides (Fig. 2), and 45% *gg* and 55% *gt* in β-GlcNAc (*tg* assumed to be negligible),[20,24] that is, the difference in coupling does not indicate a significant difference in the rotamer populations. The $^{3}J_{2,H-N}$ couplings in HA oligosaccharides differ from those of monosaccharide GlcNAc (as reported before[11]) and also vary with residue position (see below).

Several spin systems within HA oligosaccharides have strongly coupled ^{1}H nuclei, which result in non-first-order resonance lineshapes even at 900 MHz.[19] Because vicinal $^{3}J_{H,H}$ coupling constants in GlcA and GlcNAc rings are 8–10 Hz (Table 5), adjacent nuclei with differences in chemical shift ($\Delta\delta$) less than or comparable to 0.010 ppm suffer severe second-order effects at 900 MHz. In reducing-terminal GlcNAc rings (as in **1**, **3** and **4**), nuclei H-4 and H-5 are strongly coupled ($\Delta\delta \approx 0.002$ ppm, see Tables 1–3, respectively). Oligosaccharides derived using the bacterial lyase (i.e., **6**, Δ-HA_4^{AN}) display strong-coupling between H-4 and H-5 in the GlcNAc ring preceding the non-reducing terminal Δ-4,5-GlcA residue ($\Delta\delta \approx 0.002$ ppm, see Table 2). In oligosaccharides with non-reducing terminal GlcA rings (i.e., **2**, **5** and **7**), nuclei H-3 and H-4 are also severely strongly coupled ($\Delta\delta \approx 0.001$ ppm, see Tables 1–3, respectively). It is important to note that it is not just the strongly coupled protons that suffer non-first-order distortions because other protons coupled to the strongly coupled pair also display perturbed multiplets via 'virtual' coupling.[25] For example, the H-2^{VI} proton (3.319 ppm) is virtually coupled to the strongly coupled H-3^{VI}/H-4^{VI} pair ($\Delta\delta \approx 0.001$ ppm) in oligosaccharide **7** (HA_6^{AN}) and has a lineshape considerably more complex than a typical quartet (see Fig. 3). The particular frequencies and intensities of the 'wings' to this resonance depend upon other vicinal couplings (i.e., $^{3}J_{3,4}$, $^{3}J_{4,5}$) in the spin system and the chemical shift difference between the strongly coupled pair.[25] This complex lineshape was readily reproduced by an NMR simulation program (GAMMA[26]) that included a full spin spin Hamiltonian (see Fig. 3), using multiple iterative rounds with floating values for $^{3}J_{H,H}$ and $\Delta\delta$(H-3,H-4) to find the best fit to the intensity data (see Section 4). The resultant $^{3}J_{H,H}$ coupling constants were not significantly different (<0.1 Hz) from those measured in other GlcA rings (Table 5) and the $\Delta\delta$(H-3,H-4) was determined to be 0.0023 ppm (i.e., both within the error of the experimental measurements made). Less severe strong coupling distortions have also been observed (at 750 MHz) in GlcA rings where the difference in frequency between H-4 and H-5 is $2–3 \times {}^{3}J_{4,5}$.[27]

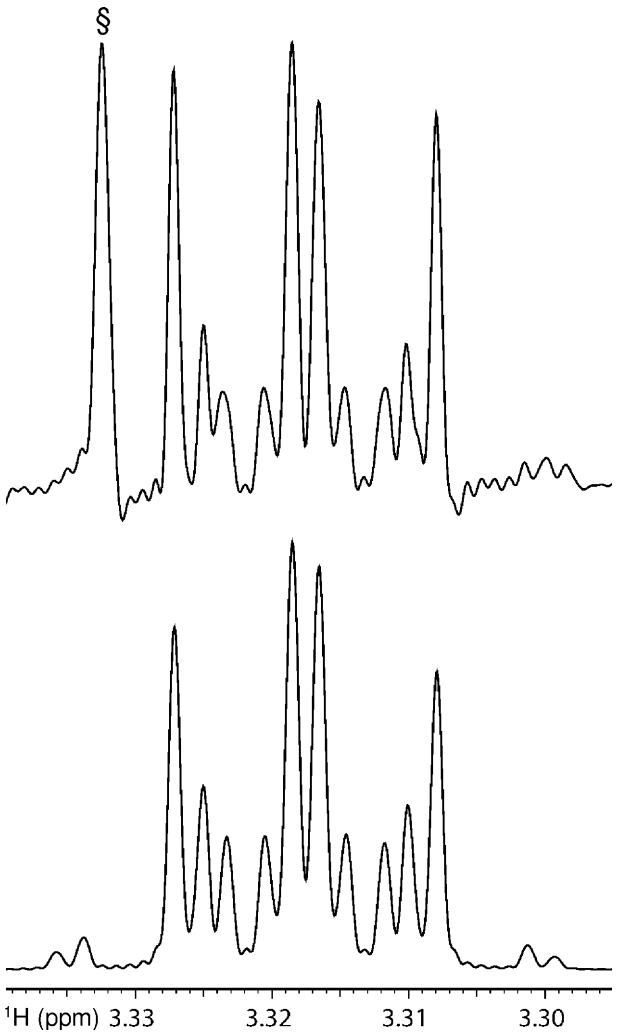

Figure 3. (Top) Resonance lineshape of the H-2^{VI} proton in oligosaccharide **7** (HA_6^{AN}). While the lineshape seems to be a simple quartet with non-first-order virtual coupling 'wings', there is no simple relationship between the line spacings and couplings.[25] The resonance indicated by § is part of the GlcA H-2^{IV} multiplet, that is, is not part of the H-2^{VI} spin system. (Bottom) Best-fit H-2^{VI} multiplet generated by simulation with the program GAMMA.[26]

2.3. Perturbations arising from different terminal saccharide rings

Differences in chemical shifts and coupling constants between GlcA and GlcNAc rings within the same oligosaccharide arise from end-effects, which include not only differences in chemical bonding (e.g., α anomers and residues with only one glycosidic linkage) but also perturbations to local dynamic motions arising from the different chemical structures.[15] In the case of ring ^{1}H and ^{13}C nuclei, end-effects are only discernible at terminal and penultimate rings (at pH 6.0, 24.4 °C and 900 MHz ^{1}H resonance frequency; see Tables 1–3). The chemical shifts of the central GlcNAc and GlcA rings of hexasaccharide **7** (rings III and IV, respectively) are therefore a good measure of the intrinsic values for GlcNAc and GlcA residues in HA polymer.[10] Comparison of these chemical shifts to those observed in each different terminus allows the end-effects to ring ^{1}H and ^{13}C chemical shifts to be quantified (Fig. 4).

The largest chemical shift perturbations are found in the terminal rings where the absence of the glycosidic linkage naturally makes a large difference. At the linkage point,^{13}C nuclei are perturbed by −5 to −11 ppm and ^{1}H nuclei −0.2 to 0.6 ppm relative to equivalent nuclei in interior rings. Directly adjacent nuclei are perturbed by an order of magnitude less (^{13}C −1.3 to 1.3 ppm) and those two bonds away by an order of magnitude less again (^{13}C −0.1 to 0.2 ppm), except in the case of the reducing terminal α-GlcA and α-GlcNAc residues, which show large differences throughout the ring; all these perturbations are typically seen with linkage changes in carbohydrate residues.

The penultimate rings have identical chemical structures to residues within HA polymer, and therefore the small differences in their chemical shifts caused by the different termini are more likely to be related to subtle changes in the local conformation (or interactions with water molecules). Residues adjacent to reducing terminal GlcNAc residues display distinct chemical shifts for α and β forms throughout the ring (see Tables 2, 3 and Fig. 4), whereas those adjacent to reducing terminal GlcA residues only display differences for the α and β forms at C-1 and H-1 (see Table 1 and Fig. 4). With a reducing terminal GlcNAc residue, the largest differences in the penultimate residues between the α and β forms are seen at H-1, C-1 and H-5. With a non-reducing terminal GlcA residue, C-3 on the adjacent GlcNAc ring (i.e., the next linkage carbon) is perturbed considerably (0.563 ppm), which is surprising as it is six chemical bonds away from the lost linkage site (i.e., C-4 on the GlcA ring); H-4 and C-4 on the adjacent GlcNAc ring are also noticeably perturbed. The hydroxymethyl protons (H6*proR*, H6*proS*) in non-reducing terminal GlcNAc residues have significantly different chemical shifts to the interior of HA. Finally, GlcNAc residues adjacent to a Δ-4,5-GlcA ring have perturbed resonances at the hydroxymethyl protons and the amide group (Fig. 5).

The amide group ^{1}H and ^{15}N nuclei are considerably more sensitive to end-effects than the ring ^{1}H and ^{13}C nuclei, with measurable perturbations at up to 3 or 4 rings from the termini; in fact, all four amide groups within the octasaccharide $HA_8{}^{AN}$ can be easily resolved at 750 MHz (see Fig. 5).[15] Previously it was proposed that the most central amide group within the decasaccharide $HA_{10}{}^{AN}$ (i.e., N–H^{V}, N^{V}) had chemical shifts (8.040 and 121.942 ppm) representative of the HA polymer,[15] and this is now confirmed by comparison with the [^{1}H–^{15}N] HSQC spectrum of the doicosasaccharide $HA_{22}{}^{AN}$ (Fig. 5) in which the interior amide resonances (from rings V–XIX) totally overlap (at 8.040 and 121.943 ppm). Non-reducing terminal Δ-4,5-GlcA residues induce a significant perturbation to the amide group in the penultimate GlcNAc residue (^{1}H 0.0091 ppm, ^{15}N 0.223 ppm). The end-effects in amide ^{1}H and ^{15}N chemical shifts due to other reducing and non-reducing termini have been described before.[15,18,28]

In the case of disaccharide **1** ($HA_2{}^{AN}$), end-effects from reducing and non-reducing terminal residues are experienced at both residues simultaneously. Simple addition of both sets of chemical shift perturbations (taken from Fig. 4) to the intrinsic values for GlcA and GlcNAc residues within the HA polymer predicts the chemical shifts for all nuclei in **1** to a reasonable accuracy (±0.006 ppm), except in the case of the linkage carbons (i.e., C-3$^{I\alpha/\beta}$, C-1^{II}) that deviate by ∼0.055 ppm. Similarly, the chemical shifts within the central ring of the trisaccharide **4** ($HA_3{}^{NN}$) are predicted to an accuracy of ±0.006 ppm (all nuclei) by simple addition of both end-effects, except in the case of the linkage carbons (∼0.060 ppm).

Differences in coupling constants arising from the various types of terminal residues were only observed for terminal GlcNAc rings (see Table 5). Specifically, the $^{3}J_{2,H-N}$ values in reducing terminal α-GlcNAc (9.5 Hz) and non-reducing terminal GlcNAc (9.4 Hz) differ from those of internal GlcNAc rings (9.7 Hz). The $^{3}J_{5,6proR}$ coupling in reducing terminal α-GlcNAc (4.9 Hz) also differs from internal GlcNAc residues (5.4 Hz), corresponding to slightly different fractional rotamer populations (52% *gg* and 48% *gt*).

3. Discussion

Simple homonuclear and ^{13}C-natural abundance spectra acquired at 900 MHz have been sufficient to allow the resolution and assignment of all ^{1}H and ^{13}C nuclei within a range of HA oligosaccharides up to the hexasaccharide **7**. End-effect perturbations to chemical shifts and coupling constants in terminal and penultimate residues

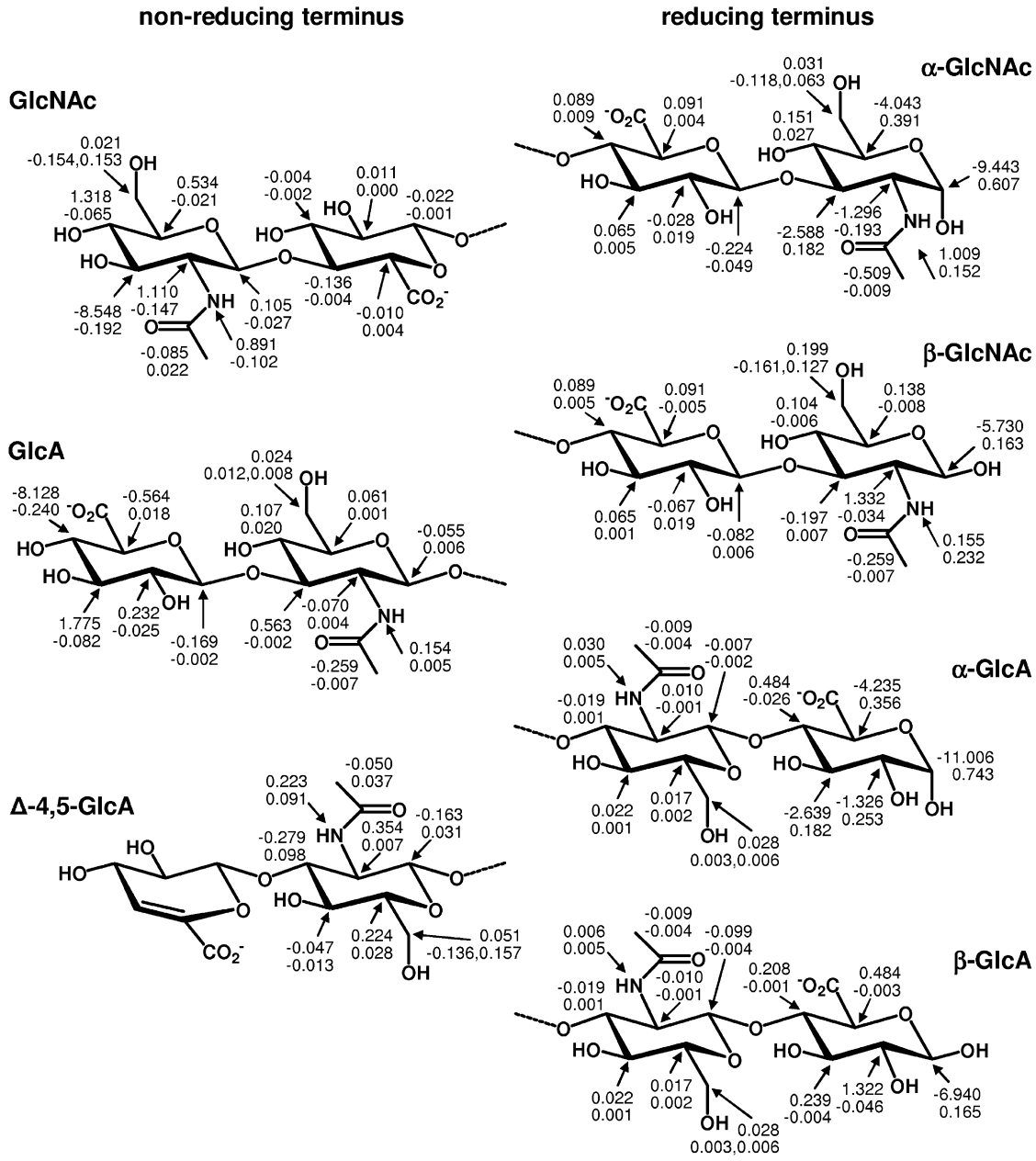

Figure 4. Chemical shift perturbations arising from different non-reducing (left) and reducing (right) termini in HA oligosaccharides. Values have been calculated for each C–H group relative to the interior GlcNAc^{III} and GlcA^{IV} rings of hexasaccharide **7** ($HA_6{}^{AN}$) and for each N–H group relative to the interior GlcNAc$^{V–XIX}$ resonances of the doicosasaccharide $HA_{22}{}^{AN}$, which are taken as representative of the intrinsic values within HA. Positive values indicate a higher chemical shift relative to the interior (i.e., lower resonant frequency) and at each centre the perturbation to the heteronucleus is the upper value. At hydroxymethyl groups, the value for H6*proR* is given first. Perturbations arising from the reducing terminal α- and β-GlcNAc and non-reducing terminal GlcA were calculated using the values for **7** (Table 3), those from reducing terminal α- and β-GlcA and non-reducing terminal GlcNAc using the chemical shifts of **3** (Table 1), and those for non-reducing terminal Δ-4,5-GlcA the chemical shifts of **6** (Table 2).

have been characterized for seven different terminal residues. Considering all these various perturbations, it is concluded that the hexasaccharide **7** $HA_6{}^{AN}$ provides the best resolution for ^1H and ^{13}C nuclei in as long a length of oligosaccharide as possible (at 900 MHz); longer molecules (such as $HA_7{}^{MN}$ or $HA_7{}^{AA}$) would result in significant overlap of one or more interior residues and thereby prevent unambiguous, sequence-specific characterization of the glycosidic linkages at the centre of the oligosaccharide.

Using the assignments in this work, it is now expected that nuclear Overhauser enhancement (NOE), rotating-frame NOE (ROE) and residual dipolar coupling (RDC) structural restraints for ring nuclei in the centre of the hexasaccharide **7** can be acquired without significant resonance overlap. These data will allow the glycosidic

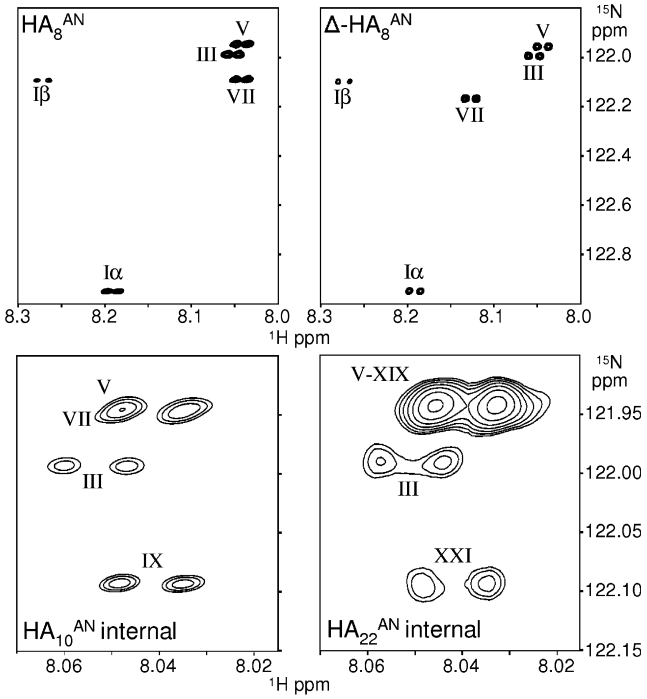

Figure 5. Selected [^{1}H–^{15}N]-HSQC spectra of HA oligosaccharides with resonance assignments indicated. (Top) Comparison of the full spectra of the octasaccharides HA_8^{AN} and Δ-HA_8^{AN}, showing the perturbation to the amide on ring VII caused by the different non-reducing terminal residue. (Bottom) Comparison of the internal amide resonances of HA_{10}^{AN} and HA_{22}^{AN}. The most interior amide within HA_{10}^{AN} (i.e., that on ring V) has the same chemical shifts as those in HA_{22}^{AN}, indicating that it does not experience measurable end-effects.

linkages and sidechain orientations to be precisely characterized and extrapolated to models for the polymer, as has already been performed using data acquired solely on HA amide groups.[11,16] It is also expected that comparisons of NOE patterns from different terminal rings will aid the assignment of NOEs in **7** (HA_6^{AN}) where ^{1}H resonances are resolved but nevertheless ambiguous in the absence of other data.

The unique chemical structures associated with the terminal residues of oligosaccharides (i.e., α- and β-anomers at reducing termini and the absence of one glycosidic linkage in each terminal residue relative to the polymer; see Fig. 4) are likely to underpin the differences between oligomeric and polymeric HA. In this regard, the various different terminal residues result in several interesting perturbations to coupling constants (i.e., the amide and hydroxymethyl sidechains) and chemical shifts (e.g., H-4 in GlcNAc rings penultimate to non-reducing terminal GlcA). These differences are likely to be arising from a combination of several effects, including changes in local hydrogen-bonding arrangements, dynamic motions and interactions with water molecules. The accuracy with which the chemical shifts of the very short oligosaccharides (i.e., di- and trisaccharides) could be predicted by simple combination of the relevant end-effects implies that the phenomena generating these differences are quite discrete. A molecular account of these perturbations awaits further structural data, comparison with MD simulations and ab initio calculations of chemical shifts.

The ^{1}H and ^{13}C assignments presented here for the tetrasaccharide **5** (HA_4^{AN}) at pH 6.0 in H_2O are in complete agreement with those determined at pH 5.6 in D_2O by Toffanin and colleagues,[9] once deuterium isotope-effects and the different reference compound (internal acetone) have been accounted for. The majority of assignments made for **5** (HA_4^{AN}) at pH 3.3 in D_2O reported by Livant and colleagues[12] are consistent with those presented here, except that for H-5$^{I\alpha}$ which we believe to be misassigned due to the resonance overlap with H-3$^{I\alpha}$ (and not H-5$^{III\beta}$ as Livant proposed). The anomeric twinning seen at H-1^{III} at pH 3.3, which was discounted as an artefact by Toffanin and colleagues, is likely to be correct as a similar effect is seen for the H–N^{III} and N^{III} nuclei at pH 3.0 (i.e. at the pK_a value of GlcA carboxylate groups in HA). This effect is likely to be mediated by a through-space effect caused by a subtle difference in pK_a value of the carboxylate group in rings IIα versus IIβ.[11] The C-2 and C–Me chemical shifts for the hexasaccharide **7** agree with those measured using an HNCA experiment on [^{15}N,^{13}C]-labelled hexasaccharides,[15] but the precision of the chemical shifts reported here is considerably better (an error of ±0.004 ppm rather than ±0.04 ppm).

The experimental methodology and data presented in this paper provide a firm foundation upon which to acquire sufficient sequence-specific data to be able to determine a representative dynamic solution conformation of HA oligosaccharides. Moreover, they provide a good first-step towards detailed characterization of the solution conformation of the polymer. Ultimately, such solution conformations will considerably aid our understanding of oligomer and polymer HA biology in health and disease.

4. Experimental

4.1. Preparation of NMR samples

Odd- and even-numbered hyaluronan oligosaccharides were prepared as described previously,[11,15,18,29] that is, using appropriate combinations of enzymatic and chemical reactions to degrade high molecular weight HA (M_r 0.5–1.5 × 10^6, from Genzyme in Boston, USA) to the desired length.

Oligosaccharide samples were prepared from lyophilised material reconstituted in 10% (v/v) D_2O, 0.02% (w/v) NaN_3, 0.3 mM DSS, pH 6.0, with the exception of those used for [^{1}H–^{15}N]-HSQC spectra (5% D_2O) and that used for assignment of oligosaccharide **2**

(100% D_2O, pH* 6.0). [^{1}H–^{1}H]-DQF-COSY, [^{1}H–^{1}H]-TOCSY and [^{1}H–^{13}C]-HSQC spectra were acquired on samples of concentrations ranging from 5 to 20 mM, while [^{1}H–^{15}N]-HSQC spectra were recorded on samples of a wider concentration range (4–35 mM, corresponding to ^{15}N concentrations of 12–105 μM at natural abundance).

4.2. Data acquisition

Experiments were performed at 24.4 °C (calibrated against methanol) at ^{1}H resonance frequencies of either 899.9 (Varian INOVA 900) or 750.0 MHz (Oxford Instruments magnet with home-built probe) using States-TPPI quadrature detection.

At 900 MHz, [^{1}H]-1D spectra were acquired over 16384 complex points with a dwell-time of 68.9 μs. All homonuclear [^{1}H–^{1}H]-2D spectra were recorded with 2048 complex points at a dwell time of 92.5 μs in the acquisition dimension (t_2). In the indirect dimension, [^{1}H–^{1}H]-DQF-COSY, [^{1}H–^{1}H]-Z-filtered-TOCSY and [^{1}H–^{1}H]-NOESY spectra were collected with a dwell-time of 119.0 μs and 768, 1024 and 256 complex points, respectively. Mixing-times used were 53 ms (TOCSY) and 400 ms (NOESY). Gradient-selective and sensitivity-enhanced [^{1}H–^{13}C]-HSQC spectra were recorded at ^{13}C-natural abundance with the τ-delay ($1/4J$) set to 1750 μs, ^{13}C carrier offset set to 70.0 ppm and dwell-times of 110.5 μs (t_1, corresponding to a sweepwidth of 40 ppm, 400 complex points) and 92.5 μs (t_2, 1024 complex points); these parameters achieved optimal resolution whilst folding the C-1 and C–Me resonances once.[30] A [^{1}H–^{13}C]-HSQC spectrum was recorded on a sample of **7** (HA_6^{AN}) with ^{13}C-broadband decoupling disabled during acquisition (which also allowed 2048 complex points in the acquisition dimension to be taken).

Gradient-enhanced [^{1}H–^{15}N]-HSQC datasets were collected at 750 MHz with many repetitions using natural abundance ^{15}N (~0.3%) as described before.[18] A [^{1}H–^{15}N]-HSQC spectrum was recorded on the ^{15}N-labelled sample of **5** (HA_4^{AN}) prepared previously[15] with the τ-delay ($1/4J$) set to 25 ms, which allowed resonances correlating the methyl proton to the nitrogen in each acetamido sidechain to be observed.

4.3. Data processing, referencing and analysis

Spectra were processed using NMRPipe[31] as detailed previously,[11,15,19] that is, using appropriate linear prediction, window functions (cosine-bell and Lorentz-to-Gauss apodizations) and zero-filling to obtain the maximum resolution possible from each dataset.

Proton chemical shifts were referenced relative to internal DSS (2,2-dimethyl-2-silapentane-5-sulfonate, non-deuterated), giving a standard error for $\delta_{DSS}(^1H)$ of ±0.001 ppm for ^{1}H resonances between different samples of the same oligosaccharide. The heteronuclei were referenced indirectly using the consensus frequency ratios[32] uncorrected for the (small) temperature difference from 24.4 °C. Under the sample conditions used in this work, the ^{13}C chemical shift of the DSS degenerate methyl groups in [^{1}H–^{13}C]–HSQC spectra was found to be at -0.004 ± 0.003 ppm in 100% D_2O samples, and at 0.067 ± 0.004 ppm in 5% and 10% D_2O samples. No chemical shift perturbations to DSS or HA oligosaccharides were seen upon addition of DSS to oligosaccharides, that is, indicating they do not associate. Chemical shifts reported are those of the centre of mass of each multiplet, uncorrected for perturbations arising from strong coupling. Spectra were also analysed to determine if the linear prediction used affected the accuracy of the reported chemical shifts; no differences in chemical shifts were detectable (i.e., <1 ppb) between datasets processed with or without linear prediction.

Spectra were analysed with NMRPipe and Sparky.[33] The $^3J_{H,H}$ and $^1J_{C,H}$ coupling constants were determined by direct measurement from the high-resolution [^{1}H]-1D and ^{13}C-decoupled [^{1}H–^{13}C]-HSQC spectra, respectively.

4.4. Simulation of virtual coupling wings

The non-first-order lineshape of the H-2^{VII} proton in oligosaccharide **7** (HA_6^{AN}) was simulated using the program GAMMA.[26] All five protons within the GlcA ring (i.e., H-1^{VII}, H-2^{VII}, H-3^{VII}, H-4^{VII}, H-5^{VII}) were used to model the spin system, with chemical shifts and $^3J_{H,H}$ couplings between them being initially set to the measured values (Tables 3 and 4). 1D-Spectra were simulated (by applying a single perfect 90° pulse) and processed with identical parameters to those used experimentally (see above). All $^3J_{H,H}$ couplings and the difference between the H-4^{VII} and H-5^{VII} chemical shifts were allowed to vary until the best-fit (χ^2) to the experimental data was obtained.

Acknowledgements

A.A. and C.D.B. were funded by a BBSRC Sir David Phillips research fellowship, while MACR was supported by the HEFCE. The Varian INOVA 900 MHz NMR spectrometer was from the Henry Wellcome Building for Biomolecular NMR Spectroscopy, University of Birmingham, UK, whilst the 750 MHz spectrometer was from the Oxford Centre for Molecular Sciences, University of Oxford, UK. We thank Professors Michael Overduin (Birmingham) and Iain Campbell (Oxford) for their generous provision of the use of these facilities. We are grateful to Professor Paul DeAngelis (University of Oklahoma, OK, USA) for helping to

generate the ^{15}N-labelled $HA_4{}^{AN}$ sample and Dr. Simon Colebrooke (Oxford) for his technical assistance.

Supplementary data

Supplementary data associated with this article can be found, in the online version, at doi:10.1016/j.carres.2006.09.023.

References

1. Day, A. J.; Prestwich, G. D. *J. Biol. Chem.* **2002**, *277*, 4585–4858.
2. Day, A. J.; de la Motte, C. A. *Trends. Immunol.* **2005**, *26*, 637–643.
3. Straach, K. J.; Shelton, J. M.; Richardson, J. A.; Hascall, V. C.; Mahendroo, M. S. *Glycobiology* **2005**, *15*, 55–65.
4. Felszeghy, S.; Meszar, Z.; Prehm, P.; Modis, L. *Arch. Oral. Biol.* **2005**, *50*, 175–179.
5. Yabushita, H.; Kishida, T.; Fusano, K.; Kanyama, K.; Zhuo, L.; Itano, N.; Kimata, K.; Noguchi, M. *Oncol. Rep.* **2005**, *13*, 1101–1105.
6. Chai, S.; Chai, Q.; Danielsen, C. C.; Hjorth, P.; Nyengaard, J. R.; Ledet, T.; Yamaguchi, Y.; Rasmussen, L. M.; Wogensen, L. *Circ. Res.* **2005**, *96*, 583–591.
7. Stern, R.; Asari, A. A.; Sugahara, K. N. *Eur. J. Cell Biol.* **2006**, *85*, 699–715.
8. Cowman, M. K.; Matsuoka, S. *Carbohydr. Res.* **2005**, *340*, 791–809.
9. Toffanin, R.; Kvam, B. J.; Flaibani, A.; Atzori, M.; Biviano, F.; Paoletti, S. *Carbohydr. Res.* **1993**, *245*, 113–128.
10. Cowman, M. K.; Hittner, D. M.; FederDavis, J. *Macromolecules* **1996**, *29*, 2894–2902.
11. Blundell, C. D.; DeAngelis, P. L.; Almond, A. *Biochem. J.* **2006**, *396*, 487–498.
12. Livant, P.; Roden, L.; Krishna, N. R. *Carbohydr. Res.* **1992**, *237*, 271–281.
13. Sicinska, W.; Adams, B.; Lerner, L. *Carbohydr. Res.* **1993**, *242*, 29–51.
14. Holmbeck, S. M.; Petillo, P. A.; Lerner, L. E. *Biochemistry* **1994**, *33*, 14246–14255.
15. Blundell, C. D.; DeAngelis, P. L.; Day, A. J.; Almond, A. *Glycobiology* **2004**, *14*, 999–1009.
16. Almond, A.; DeAngelis, P. L.; Blundell, C. D. *J. Mol. Biol.* **2006**, *358*, 1256–1269.
17. Almond, A.; DeAngelis, P. L.; Blundell, C. D. *J. Am. Chem. Soc.* **2005**, *127*, 1086–1087.
18. Blundell, C. D.; Almond, A. *Anal. Biochem.* **2006**, *353*, 236–247.
19. Blundell, C. D.; Reed, M. A.; Overduin, M.; Almond, A. *Carbohydr. Res.* **2006**, *341*, 1985–1991.
20. Nishida, Y.; Hori, H.; Ohrui, H.; Meguro, H. *Carbohydr. Res.* **1987**, *170*, 106–111.
21. Yates, E. A.; Santini, F.; De Cristofano, B.; Payre, N.; Cosentino, C.; Guerrini, M.; Naggi, A.; Torri, G.; Hricovini, M. *Carbohydr. Res.* **2000**, *329*, 239–247.
22. Coxon, B. *Carbohydr. Res.* **2005**, *340*, 1714–1721.
23. Gettins, P.; Horne, A. P. *Carbohydr. Res.* **1992**, *223*, 81–98.
24. Haasnoot, C. A. G.; Deleeuw, F. A. A. M.; Altona, C. *Tetrahedron* **1980**, *36*, 2783–2792.
25. Musher, J. I.; Corey, E. J. *Tetrahedron* **1962**, *18*, 791–797.
26. Smith, S. A.; Levante, T. O.; Meier, B. H.; Ernst, R. R. *J. Magn. Reson. Ser. A* **1994**, *106*, 75–105.
27. Colebrooke, S. A.; Blundell, C. D.; DeAngelis, P. L.; Campbell, I. D.; Almond, A. *Magn. Reson. Chem.* **2005**, *43*, 805–815.
28. Cowman, M. K.; Cozart, D.; Nakanishi, K.; Balazs, E. A. *Arch. Biochem. Biophys.* **1984**, *230*, 203–212.
29. Seyfried, N. T.; Blundell, C. D.; Day, A. J.; Almond, A. *Glycobiology* **2005**, *15*, 303–312.
30. Blundell, C. D.; Almond, A.; Mahoney, D. J.; DeAngelis, P. L.; Campbell, I. D.; Day, A. J. *J. Biol. Chem.* **2005**, *280*, 18189–18201.
31. Delaglio, F.; Grzesiek, S.; Vuister, G. W.; Zhu, G.; Pfeifer, J.; Bax, A. *J. Biomol. NMR* **1995**, *6*, 277–293.
32. Wishart, D. S.; Bigam, C. G.; Yao, J.; Abildgaard, F.; Dyson, H. J.; Oldfield, E.; Markley, J. L.; Sykes, B. D. *J. Biomol. NMR* **1995**, *6*, 135–140.
33. Goddard, T. D.; Kneller, D. G. SPARKY 3 University of California, San Francisco.